ARCHIVUM MATHEMATICUM (BRNO)
Tomus 59 (2023), 263–274

AN UNCONDITIONALLY STABLE FINITE ELEMENT SCHEME FOR ANISOTROPIC CURVE SHORTENING FLOW

Klaus Deckelnick and Robert Nürnberg

Abstract. Based on a recent novel formulation of parametric anisotropic curve shortening flow, we analyse a fully discrete numerical method of this geometric evolution equation. The method uses piecewise linear finite elements in space and a backward Euler approximation in time. We establish existence and uniqueness of a discrete solution, as well as an unconditional stability property. Some numerical computations confirm the theoretical results and demonstrate the practicality of our method.

1. Introduction

In this paper we study a fully discrete numerical scheme for parametric anisotropic curve shortening flow. This evolution law arises as a natural gradient flow for the energy

$$\mathcal{E}(\Gamma) = \int_\Gamma a(z)\gamma(z,\nu)\,\mathrm{d}\mathcal{H}^1(z) = \int_\Gamma a\,\gamma(\cdot,\nu)\,\mathrm{d}\mathcal{H}^1\,, \tag{1.1}$$

where Γ is a closed curve with unit normal ν contained in a given convex domain $\Omega \subset \mathbb{R}^2$. Furthermore, $a \in C^1(\Omega, \mathbb{R}_{>0})$ is a weight function and $\gamma \in C^0(\Omega \times \mathbb{R}^2, \mathbb{R}_{\geq 0}) \cap C^2(\Omega \times (\mathbb{R}^2 \setminus \{0\}), \mathbb{R}_{>0})$ denotes an anisotropy function satisfying

$$\gamma(z,\lambda p) = |\lambda|\gamma(z,p) \quad \text{for all } p \in \mathbb{R}^2,\ \lambda \in \mathbb{R},\ z \in \Omega\,. \tag{1.2}$$

In addition, we assume that γ is strictly convex in the sense that for every compact $K \subset \Omega$ there exists $c_K > 0$ such that

$$\gamma_{pp}(z,p)q\cdot q \geq c_K|q|^2 \quad \text{for all } z \in K,\ p,q \in \mathbb{R}^2 \text{ with } p\cdot q = 0, |p| = 1.$$

Here, and in what follows, γ_p and γ_{pp} denote gradient and Hessian of the function $p \mapsto \gamma(\cdot,p)$. Anisotropic energies of the form (1.1) play a role in applications, such as materials science, crystal growth, phase transitions and image processing, and in differential geometry, and we refer to e.g. [1, 9, 10, 12, 13, 23, 24, 25, 32] for examples

2020 *Mathematics Subject Classification*: primary 65M60; secondary 65M12, 53E10, 35K15.
Key words and phrases: anisotropic curve shortening flow, finite element method, stability.
Received September 16, 2022, accepted November 210, 2022. Editor P. Krejčí.
DOI: 10.5817/AM2023-3-263

and further details. It can be shown, see [16, Appendix A], that the first variation of $\mathcal{E}$ in the direction of a smooth vector field V is given by

$$d\mathcal{E}(\Gamma; V) = -\int_\Gamma a\,\gamma(\cdot,\nu)\,\varkappa_\gamma\,V\cdot\nu_\gamma \,\mathrm{d}\mathcal{H}^1\,, \tag{1.3}$$

where

$$\nu_\gamma = \frac{\nu}{\gamma(\cdot,\nu)} \quad\text{and}\quad \varkappa_\gamma = \varkappa\gamma_{pp}(\cdot,\nu)\tau\cdot\tau - \sum_{i=1}^{2}\gamma_{p_i z_i}(\cdot,\nu) - \frac{\nabla a}{a}\cdot\gamma_p(\cdot,\nu) \quad \text{on } \Gamma$$

denote the anisotropic normal and the anisotropic curvature of Γ, respectively, with τ and $\varkappa$ the tangent and curvature of Γ.

In view of (1.3), a natural gradient flow for the energy $\mathcal{E}$ evolves a family of closed curves $(\Gamma(t))_{t\in[0,T]}$ according to

$$\mathcal{V}_\gamma = \varkappa_\gamma \quad \text{on } \Gamma(t)\,, \tag{1.4}$$

where $\mathcal{V}_\gamma = \frac{1}{\gamma(\cdot,\nu)}\mathcal{V}$ and $\mathcal{V}$ is the normal velocity of $\Gamma(t)$. We remark that solutions of (1.4) satisfy the energy relation

$$\frac{\mathrm{d}}{\mathrm{d}t}\int_{\Gamma(t)} a\,\gamma(\cdot,\nu)\,\mathrm{d}\mathcal{H}^1 + \int_{\Gamma(t)} |\mathcal{V}_\gamma|^2\,a\,\gamma(\cdot,\nu)\,\mathrm{d}\mathcal{H}^1 = 0\,.$$

Note that in the isotropic case, $a(z) = 1$ and $\gamma(z,p) = |p|$, the flow (1.4) collapses to the well–known curve shortening flow $\mathcal{V} = \varkappa$. The isotropic curve shortening flow and its higher dimensional analogue, the mean curvature flow, have been studied extensively both analytically and numerically over the last few decades, and we refer to the works [8, 15, 20, 27] for more details.

In the spatially homogeneous case, $a(z) = 1$ and $\gamma(z,p) = \gamma_0(p)$, the flow (1.4) reduces to the classical anisotropic curve shortening flow

$$\frac{1}{\gamma_0(\nu)}\mathcal{V} = \varkappa_{\gamma_0}\,, \tag{1.5}$$

where $\varkappa_{\gamma_0} = \varkappa\gamma_0''(\nu)\tau\cdot\tau$ denotes the usual anisotropic curvature. An example for a nonconstant function a is given by the geodesic curvature flow in a Riemannian manifold, see §3.2 and [16, Appendix B] for details.

In this paper we focus on a parametric description of the evolving curves, i.e. $\Gamma(t) = x(I,t)$ with $x\colon I\times[0,T]\ni(\rho,t)\mapsto x(\rho,t)\in\mathbb{R}^2$ and $I = \mathbb{R}/\mathbb{Z}$. Hence the evolution law (1.4) translates into

$$\frac{1}{\gamma(x,\nu)}x_t\cdot\nu = \varkappa_\gamma\,, \tag{1.6}$$

where $\nu = \tau^\perp = (\frac{x_\rho}{|x_\rho|})^\perp$ and $p^\perp = \binom{p_1}{p_2}^\perp = \binom{-p_2}{p_1}$ denotes an anti-clockwise rotation of p by $\frac{\pi}{2}$. Note that here, and from now on, we think of τ, ν, $\varkappa$ and $\varkappa_\gamma$ as being defined on $I\times[0,T]$.

In order to obtain solutions of (1.6), frequently the partial differential equation (PDE) given by

$$\frac{1}{\gamma(x,\nu)}x_t = \varkappa_\gamma\nu \tag{1.7}$$

is solved, with the initial condition $x(\cdot,0) = x_0$, where x_0 is a parameterization of the initial curve Γ_0. Since the right hand side of (1.7) is a geometric invariant, the above PDE appears to be a natural choice. Let us focus for a moment on the isotropic case $a(z) = 1$ and $\gamma(z,p) = |p|$. Then the system (1.7) takes the form

$$x_t = \varkappa\nu = \frac{1}{|x_\rho|}\left(\frac{x_\rho}{|x_\rho|}\right)_\rho = \frac{1}{|x_\rho|^2}\left[x_{\rho\rho} - (x_{\rho\rho}\cdot\tau)\,\tau\right], \tag{1.8}$$

so that the underlying PDE is only weakly parabolic, causing difficulties for the numerical analysis. We refer to Dziuk's seminal paper [18] for the details. A simple remedy is to apply the so-called DeTurck trick, and to consider, in place of (1.8), the strictly parabolic PDE

$$x_t = \frac{x_{\rho\rho}}{|x_\rho|^2}\,, \tag{1.9}$$

whose solutions clearly still satisfy $x_t\cdot\nu = \varkappa$. This formulation was proposed and analysed for the first time in [14], see also [21] for a possible generalization.

Extending the DeTurck trick (1.9) for the isotropic flow to the anisotropic evolution equation (1.6) is highly nontrivial. However, the main idea is the same: derive a strictly parabolic PDE whose solutions satisfy (1.6). In this way, a uniquely defined tangential velocity is prescribed together with the normal velocity (1.6), yielding a unique parameterization of the evolving curve. In fact, in the recent paper [16], the authors proved that solutions to the strictly parabolic PDE

$$H(x,x_\rho)x_t = [\Phi_p(x,x_\rho)]_\rho - \Phi_z(x,x_\rho) \tag{1.10}$$

also satisfy (1.6). Here

$$\Phi(z,p) = \tfrac{1}{2}a^2(z)\gamma^2(z,p^\perp)\,, \tag{1.11}$$

with Φ_z denoting the gradient of $z\mapsto\Phi(z,\cdot)$, and the matrix

$$H(z,p) = \frac{a^2(z)\gamma(z,p^\perp)}{|\gamma_p(z,p^\perp)|^2}\begin{pmatrix}\gamma(z,p^\perp) & \gamma_p(z,p^\perp)\cdot p\\ -\gamma_p(z,p^\perp)\cdot p & \gamma(z,p^\perp)\end{pmatrix} \quad \forall\, z\in\Omega,\ p\in\mathbb{R}^2\setminus\{0\}$$

is positive definite in $\Omega\times(\mathbb{R}^2\setminus\{0\})$ with

$$H(z,p)\xi\cdot\xi = \frac{a^2(z)\gamma^2(z,p^\perp)}{|\gamma_p(z,p^\perp)|^2}|\xi|^2 \quad \forall\, z\in\Omega,\ p\in\mathbb{R}^2\setminus\{0\},\ \xi\in\mathbb{R}^2\,. \tag{1.12}$$

The weak formulation of (1.10) is obtained by multiplying it with a test function, integrating over I and performing one integration by parts. It reads as follows. Given $x_0 : I\to\Omega$, find $x : I\times[0,T]\to\Omega$ such that $x(\cdot,0) = x_0$ and, for $t\in(0,T]$,

$$\int_I H(x,x_\rho)x_t\cdot\eta\,\mathrm{d}\rho + \int_I \Phi_p(x,x_\rho)\cdot\eta_\rho\,\mathrm{d}\rho + \int_I \Phi_z(x,x_\rho)\cdot\eta\,\mathrm{d}\rho = 0 \quad \forall\,\eta\in[H^1(I)]^2\,. \tag{1.13}$$

For a continuous-in-time semidiscrete finite element approximation of (1.13) using piecewise linear elements the authors were then able to prove an optimal H^1–error bound, see [16, Theorem 4.1].

In this paper we propose and analyse a fully discrete finite element approximation of (1.13). The scheme, which will be introduced in Section 2, is nonlinear and uses both explicit and implicit approximations in $\Phi_p(x,x_\rho)$ and $\Phi_z(x,x_\rho)$ that are chosen in such a way as to yield unconditional stability. Here the discrete stability bound will mimic the natural estimate

$$\frac{\mathrm{d}}{\mathrm{d}t}\int_I \Phi(x,x_\rho)\,\mathrm{d}\rho = -\int_I H(x,x_\rho)x_t\cdot x_t\,\mathrm{d}\rho \le 0\,,$$

which follows from choosing $\eta = x_t$ in (1.13). Furthermore, we prove the existence of a unique solution under a suitable CFL condition. Then in Section 3 we present some numerical simulations, demonstrating the practicality of the method, as well as the good properties with respect to stability and the distribution of vertices. Let us finally mention that alternative numerical approximations of anisotropic variants of curve shortening flow, which are based on a parametric description of the moving curve, have also been considered in [3, 4, 5, 7, 11, 19, 26, 28, 29, 30, 31].

2. Finite element approximation

Let $[0,1] = \bigcup_{j=1}^J I_j$, $J \ge 3$, be a decomposition of $[0,1]$ into the intervals $I_j = [q_{j-1}, q_j]$, where, for simplicity, $q_j = jh$, $j = 0,\ldots,J$, with $h = \frac{1}{J}$. Within I we identify $q_J = 1$ with $q_0 = 0$ and define the finite element space $\underline{V}^h = \{\chi \in C^0(I,\mathbb{R}^2) : \chi\,|_{I_j} \text{ is affine},\ j = 1,\ldots,J\}$. For two piecewise continuous functions, with possible jumps at the nodes $\{q_j\}_{j=1}^J$, we define the mass lumped L^2–inner product

$$(u,v)^h = \tfrac12 \sum_{j=1}^J h_j\left[(u\cdot v)(q_j^-) + (u\cdot v)(q_{j-1}^+)\right]\,, \tag{2.1}$$

where $(u\cdot v)(q_j^\pm) = \lim\limits_{\delta\searrow 0}\,(u\cdot v)(q_j \pm \delta)$. We define the associated norm on $\underline{V}^h$ via $\|u\|_h^2 = (u,u)^h$.

In order to discretize in time, let $t_m = m\Delta t$, $m = 0,\ldots,M$, with the uniform time step $\Delta t = \frac{T}{M} > 0$. On recalling (1.11), we assume that there exists a splitting $\Phi = \Phi^+ + \Phi^-$ such that $\Phi^\pm \in C^1(\Omega\times\mathbb{R}^2)$ and $z \mapsto \pm\Phi^\pm(z,p)$ are convex in Ω for all $p\in\mathbb{R}^2$. Furthermore, we assume that for every compact set $K \subset \Omega$ there exists $L_K \ge 0$ such that

$$|\Phi_z^\pm(z,p) - \Phi_z^\pm(z,q)| \le L_K(|p|+|q|)|p-q| \quad \text{for all } z\in K,\ p,q\in\mathbb{R}^2\,. \tag{2.2}$$

Then our finite element scheme is defined as follows. Given $x_h^m \in \underline{V}^h$ with $\Gamma_h^m := x_h^m(I) \subset \Omega$, for $m = 0,\ldots,M-1$, find $x_h^{m+1} \in \underline{V}^h$ such that $\Gamma_h^{m+1} \subset \Omega$ and

$$\begin{aligned}\frac{1}{\Delta t}\left(H(x_h^m, x_{h,\rho}^m)(x_h^{m+1} - x_h^m), \eta_h\right)^h &+ \left(\Phi_p(x_h^m, x_{h,\rho}^{m+1}), \eta_{h,\rho}\right)^h \\ &+ \left(\Phi_z^+(x_h^{m+1}, x_{h,\rho}^{m+1}) + \Phi_z^-(x_h^m, x_{h,\rho}^{m+1}), \eta_h\right)^h = 0 \qquad \forall\ \eta_h\in\underline{V}^h\,.\end{aligned} \tag{2.3}$$

The convex/concave splitting employed for the implicit/explicit approximation of $\Phi_z(\cdot, x_{h,\rho}^{m+1})$ in (2.3), is by now standard practice in the numerical analysis community. This technique goes back to [22], see also [2, 6, 7, 16] for subsequent applications of such splittings. It leads to an unconditionally stable approximation, as we show in our first result.

Theorem 2.1. *Any solution of* (2.3) *satisfies the energy estimate*

$$\Big(\Phi(x_h^{m+1}, x_{h,\rho}^{m+1}), 1\Big)^h + \frac{1}{\Delta t}\left(H(x_h^m, x_{h,\rho}^m)(x_h^{m+1} - x_h^m), x_h^{m+1} - x_h^m\right)^h \leq \left(\Phi(x_h^m, x_{h,\rho}^m), 1\right)^h . \tag{2.4}$$

Proof. From the convexity properties of Φ and $\pm\Phi^{\pm}$ we infer that

$$\begin{aligned}
\left(\Phi_p(x_h^m, x_{h,\rho}^m + \eta_{h,\rho}), \eta_{h,\rho}\right)^h &\geq \left(\Phi(x_h^m, x_{h,\rho}^m + \eta_{h,\rho}), 1\right)^h - \left(\Phi(x_h^m, x_{h,\rho}^m), 1\right)^h ,\\
\left(\Phi_z^+(x_h^m + \eta_h, x_{h,\rho}^m + \eta_{h,\rho}), \eta_h\right)^h &\geq \left(\Phi^+(x_h^m + \eta_h, x_{h,\rho}^m + \eta_{h,\rho}), 1\right)^h \\
&\quad - \left(\Phi^+(x_h^m, x_{h,\rho}^m + \eta_{h,\rho}), 1\right)^h ,\\
\left(\Phi_z^-(x_h^m, x_{h,\rho}^m + \eta_{h,\rho}), \eta_h\right)^h &\geq \left(\Phi^-(x_h^m + \eta_h, x_{h,\rho}^m + \eta_{h,\rho}), 1\right)^h \\
&\quad - \left(\Phi^-(x_h^m, x_{h,\rho}^m + \eta_{h,\rho}), 1\right)^h ,
\end{aligned} \tag{2.5}$$

for all $\eta_h \in \underline{V}^h$. Choosing $\eta_h = x_h^{m+1} - x_h^m$ in (2.3) and applying (2.5) yields the bound (2.4). $\square$

We note that the fully discrete finite element approximation (2.3) can be seen as a generalization of two fully discrete schemes introduced by the authors in [16]. In particular, in the special case of a spatially homogeneous anisotropy, recall (1.5), the scheme (2.3) reduces to [16, (5.4)]. Similarly, in the case when (1.6) models geodesic flow in a Riemannian manifold, the approximation [16, (5.10)] is a special case of the scheme (2.3). Moreover, we remark that the nonlinear systems of equations arising from (2.3) can be solved with a Newton method or with a Picard-type iteration. In our experience, in general, in practice these solution methods converge within a few iterations.

Let us next address the existence and uniqueness for the nonlinear system (2.3). We assume that $x_h^m \in \underline{V}^h$ is given with $x_{h,\rho}^m \neq 0$ in I and $\Gamma_h^m \subset \Omega$. There exists $R > 0$ such that $K_0 := \{z \in \mathbb{R}^2 : \operatorname{dist}(z, \Gamma_h^m) \leq R\} \subset \Omega$. Before we present our main theorem, we collect the following auxiliary results.

Lemma 2.2. *There exists a constant* $C_0 > 0$ *depending on* x_h^m *such that*

$$\Phi(z,p) \geq C_0 |p|^2 \qquad \forall\, p \in \mathbb{R}^2, z \in K_0\,, \tag{2.6a}$$

$$\big(\Phi_p(z,q) - \Phi_p(z,p)\big) \cdot (q-p) \geq C_0 |q-p|^2 \qquad \forall\, p,q \in \mathbb{R}^2, z \in K_0\,, \tag{2.6b}$$

$$H(x_h^m, x_{h,\rho}^m)\xi \cdot \xi \geq C_0 |\xi|^2 \qquad \forall\, \xi \in \mathbb{R}^2 \quad \textit{in } I\,. \tag{2.6c}$$

Proof. The bound (2.6a) follows from (1.2) and $\Phi(z,p) > 0$ for $z \in K_0$ and $|p| = 1$. Similarly, we have from (1.12) and $\min_I |x_{h,\rho}^m| > 0$ that (2.6c) holds.

It remains to show (2.6b). Since $a \geq a_0 > 0$ in K_0, it is sufficient to carry out the proof for $\Phi(z,p) = \frac{1}{2}\gamma^2(z,p)$. Note that in this case $\Phi \in C^1(\Omega \times \mathbb{R}^2, \mathbb{R}_{\geq 0}) \cap C^2(\Omega \times (\mathbb{R}^2 \setminus \{0\}, \mathbb{R}_{>0})$. Furthermore, according to [24, Remark 1.7.5], $\gamma_{pp}^2(z,p) := [\gamma^2]_{pp}(z,p)$ is positive definite for $p \neq 0$. In particular, there exists $c_0 > 0$ such that

$$\gamma_{pp}^2(z,p) q \cdot q \geq c_0 |q|^2 \qquad \text{for all } z \in K_0,\ p,q \in \mathbb{R}^2, |p| = 1\,.$$

Observing that $\Phi_{pp}(z,p) = A\gamma^2_{pp}(z,p^\perp)A^T$ with $A = \begin{pmatrix} 0 & -1 \\ 1 & 0 \end{pmatrix}$, we infer that

$$\Phi_{pp}(z,p)q \cdot q = \gamma^2_{pp}(z,p^\perp)A^T q \cdot A^T q \geq c_0|A^T q|^2 = c_0|q|^2 \tag{2.7}$$

for all $z \in K_0$, p, $q \in \mathbb{R}^2$, $|p| = 1$. Let us fix $z \in K_0$ and $p, q \in \mathbb{R}^2$. We distinguish two cases:
Case 1: $sq + (1-s)p \neq 0$ *for all* $s \in [0,1]$. Then

$$\big(\Phi_p(z,q) - \Phi_p(z,p)\big)\cdot(q-p) = \int_0^1 \Phi_{pp}(z, sq+(1-s)p)(q-p)\cdot(q-p)\,\mathrm{d}s \geq c_0|q-p|^2\,,$$

using the fact that $p \mapsto \Phi_{pp}(z,p)$ is 0-homogeneous and (2.7).
Case 2: There exists $s \in [0,1]$ with $sq+(1-s)p = 0$. We may assume that $s \in [0,1)$, so that $p = -\frac{s}{1-s}q$. As $\Phi(z,\lambda q) = \lambda^2\Phi(z,q)$ for $\lambda \in \mathbb{R}$, recall (1.2), we have that $\Phi_p(z,\lambda q) = \lambda\Phi_p(z,q)$ and $\Phi_p(z,q)\cdot q = 2\Phi(z,q)$. Hence we obtain that

$$\begin{aligned}\big(\Phi_p(z,q) - \Phi_p(z,p)\big)\cdot(q-p) &= \big(\Phi_p(z,q) - \Phi_p(z,-\tfrac{s}{1-s}q)\big)\cdot\big(q + \tfrac{s}{1-s}q\big) \\ &= \big(1+\tfrac{s}{1-s}\big)^2\Phi_p(z,q)\cdot q = 2\big(1+\tfrac{s}{1-s}\big)^2\Phi(z,q) \\ &\geq 2C_0\big(1+\tfrac{s}{1-s}\big)^2|q|^2 = 2C_0|q-p|^2,\end{aligned}$$

on noting (2.6a). □

We are now in a position to prove our main result.

Theorem 2.3. *There exists* $\delta > 0$ *such that for* $\Delta t \leq \delta h$ *there is a unique element* $x_h^{m+1} \in \underline{V}^h$ *with* $\Gamma_h^{m+1} \subset K_0$ *which solves* (2.3)*. The constant* δ *depends on* R*,* C_0*,* L_{K_0} *and* $\Phi(x_h^m, x_{h,\rho}^m)$*.*

Proof. We denote by $\{\varphi_j\}_{j=1}^{2J}$ the basis of $\underline{V}^h$ satisfying $\varphi_j(q_k) = \delta_{jk}e_1$ and $\varphi_{j+J}(q_k) = \delta_{jk}e_2$ for $1 \leq j,k \leq J$, and associate with every $\alpha \in \mathbb{R}^{2J}$ the element $v_\alpha = \sum_{j=1}^{2J}\alpha_j\varphi_j \in \underline{V}^h$, so that $v_\alpha(q_j) = \binom{\alpha_j}{\alpha_{j+J}}$. We have for $|\alpha| \leq R$ and $\rho \in I$ that

$$\operatorname{dist}((x_h^m + v_\alpha)(\rho), \Gamma_h^m) \leq \|v_\alpha\|_\infty \leq |\alpha| \leq R\,,$$

so that $(x_h^m + v_\alpha)(\rho) \in K_0$. Let us next define the continuous map $F\colon \overline{B_R(0)} \times [0,1] \to \mathbb{R}^{2J}$ via

$$\begin{aligned}[F(\alpha,\lambda)]_i = {}& \frac{1}{\Delta t}\left(H(x_h^m, x_{h,\rho}^m)v_\alpha, \varphi_i\right)^h + \lambda\left(\Phi_p(x_h^m, x_{h,\rho}^m + v_{\alpha,\rho}), \varphi_{i,\rho}\right)^h \\ &+ \lambda\left(\Phi_z^+(x_h^m + v_\alpha, x_{h,\rho}^m + v_{\alpha,\rho}) + \Phi_z^-(x_h^m, x_{h,\rho}^m + v_{\alpha,\rho}), \varphi_i\right)^h\,.\end{aligned}$$

In what follows we make use of standard results for the Brouwer degree $d(f, B_R(0), 0)$ of a continuous function $f\colon \overline{B_R(0)} \to \mathbb{R}^{2J}$, if $0 \notin f(\partial B_R(0))$, see [17, Chapter 1]. Clearly, the mapping $F(\cdot,0) =: A$ is linear with

$$[A\alpha]_i = \frac{1}{\Delta t}\sum_{j=1}^{2J}\alpha_j\left(H(x_h^m, x_{h,\rho}^m)\varphi_j, \varphi_i\right)^h\,, \quad i = 1,\ldots,2J\,,$$

and invertible in view of (2.6c). Hence it follows from [17, Theorem 1.1] that

$$d(F(\cdot,0), B_R(0), 0) = d(A, B_R(0), 0) = \operatorname{sgn}\det A \neq 0\,. \tag{2.8}$$

Next, it holds for $\lambda \in [0,1]$ that

$$F(\alpha,\lambda)\cdot\alpha = \frac{1}{\Delta t}\left(H(x_h^m, x_{h,\rho}^m)v_\alpha, v_\alpha\right)^h + \lambda\left(\Phi_p(x_h^m, x_{h,\rho}^m + v_{\alpha,\rho}), v_{\alpha,\rho}\right)^h$$
$$+ \lambda\left(\Phi_z^+(x_h^m + v_\alpha, x_{h,\rho}^m + v_{\alpha,\rho}) + \Phi_z^-(x_h^m, x_{h,\rho}^m + v_{\alpha,\rho}), v_\alpha\right)^h . \tag{2.9}$$

Inserting (2.5) with $\eta_h = v_\alpha$ into (2.9) yields

$$F(\alpha,\lambda)\cdot\alpha \geq \frac{1}{\Delta t}\left(H(x_h^m, x_{h,\rho}^m)v_\alpha, v_\alpha\right)^h$$
$$+ \lambda\big(\Phi(x_h^m + v_\alpha, x_{h,\rho}^m + v_{\alpha,\rho}), 1\big)^h - \lambda\big(\Phi(x_h^m, x_{h,\rho}^m), 1\big)^h .$$

If we combine this estimate with (2.6c) we finally obtain for $|\alpha| = R$ that

$$F(\alpha,\lambda)\cdot\alpha \geq \frac{C_0}{\Delta t}\|v_\alpha\|_h^2 - \big(\Phi(x_h^m, x_{h,\rho}^m), 1\big)^h$$
$$= \frac{C_0}{\Delta t}h|\alpha|^2 - \big(\Phi(x_h^m, x_{h,\rho}^m), 1\big)^h \geq \frac{C_0 R^2}{\delta} - \big(\Phi(x_h^m, x_{h,\rho}^m), 1\big)^h$$

using (2.1) and the relation $\Delta t \leq \delta h$. By choosing δ sufficiently small we obtain $F(\alpha,\lambda)\cdot\alpha > 0$ and therefore $F(\alpha,\lambda) \neq 0$ for all $(\alpha,\lambda) \in \partial B_R(0) \times [0,1]$. Using the homotopy invariance of the Brouwer degree together with (2.8) we deduce that $d(F(\cdot,1), B_R(0), 0) = d(F(\cdot,0), B_R(0), 0) \neq 0$, so that the existence property of the degree shows that there is $\alpha \in B_R(0)$ such that $F(\alpha,1) = 0$. Clearly, $x_h^{m+1} := x_h^m + v_\alpha$ is then a solution of (2.3).

In order to prove uniqueness, suppose that x_h^{m+1}, $\tilde{x}_h^{m+1} \in \underline{V}^h$ are two solutions of (2.3) with $\Gamma_h^{m+1}, \tilde{\Gamma}_h^{m+1} \subset K_0$. To begin, we infer from (2.4) and (2.6a) that

$$C_0\|x_{h,\rho}^{m+1}\|_h^2 \leq \big(\Phi(x_h^m, x_{h,\rho}^m), 1\big)^h,\; C_0\|\tilde{x}_{h,\rho}^{m+1}\|_h^2 \leq \big(\Phi(x_h^m, x_{h,\rho}^m), 1\big)^h . \tag{2.10}$$

We have that

$$\frac{1}{\Delta t}\big(H(x_h^m, x_{h,\rho}^m)(x_h^{m+1} - \tilde{x}_h^{m+1}), \eta_h\big)^h + \Big(\Phi_p(x_h^m, x_{h,\rho}^{m+1}) - \Phi_p(x_h^m, \tilde{x}_{h,\rho}^{m+1}), \eta_{h,\rho}\Big)^h$$
$$+ \Big(\Phi_z^+(x_h^{m+1}, x_{h,\rho}^{m+1}) - \Phi_z^+(\tilde{x}_h^{m+1}, x_{h,\rho}^{m+1}), \eta_h\Big)^h$$
$$= \Big(\Phi_z^+(\tilde{x}_h^{m+1}, \tilde{x}_{h,\rho}^{m+1}) - \Phi_z^+(\tilde{x}_h^{m+1}, x_{h,\rho}^{m+1}), \eta_h\Big)^h$$
$$+ \Big(\Phi_z^-(x_h^m, \tilde{x}_{h,\rho}^{m+1}) - \Phi_z^-(x_h^m, x_{h,\rho}^{m+1}), \eta_h\Big)^h$$

for all $\eta_h \in \underline{V}^h$. Choosing $\eta = x_h^{m+1} - \tilde{x}_h^{m+1}$ we deduce with the help of (2.6c), (2.6b), (2.2), (2.10) and the convexity of $z \mapsto \Phi^+(z,p)$ that

$$\frac{C_0}{\Delta t}\|x_h^{m+1} - \tilde{x}_h^{m+1}\|_h^2 + C_0\|x_{h,\rho}^{m+1} - \tilde{x}_{h,\rho}^{m+1}\|_h^2$$
$$\leq 2L\big(\|x_{h,\rho}^{m+1}\|_h + \|\tilde{x}_{h,\rho}^{m+1}\|_h\big)\|x_{h,\rho}^{m+1} - \tilde{x}_{h,\rho}^{m+1}\|_h\|x_h^{m+1} - \tilde{x}_h^{m+1}\|_\infty$$
$$\leq 4LC_0^{-\frac{1}{2}}h^{-\frac{1}{2}}\sqrt{\big(\Phi(x_h^m, x_{h,\rho}^m), 1\big)^h}\|x_{h,\rho}^{m+1} - \tilde{x}_{h,\rho}^{m+1}\|_h\|x_h^{m+1} - \tilde{x}_h^{m+1}\|_h$$
$$\leq C_0\|x_{h,\rho}^{m+1} - \tilde{x}_{h,\rho}^{m+1}\|_h^2 + 4L^2\big(\Phi(x_h^m, x_{h,\rho}^m), 1\big)^h C_0^{-2}h^{-1}\|x_h^{m+1} - \tilde{x}_h^{m+1}\|_h^2 ,$$

with $L = L_{K_0}$. By choosing $\delta > 0$ so small that $4L^2\big(\Phi(x_h^m, x_{h,\rho}^m), 1\big)^h\,\delta < C_0^3$ we deduce that $x_h^{m+1} = \tilde{x}_h^{m+1}$. $\square$

3. Numerical results

For all our numerical simulations we use $J = 256$ and $\Delta t = 10^{-4}$. On recalling (1.1), for $\chi_h \in \underline{V}^h$ we define the discrete energy

$$\mathcal{E}^h(\chi_h) = \big(\gamma(\chi_h, \chi_{h,\rho}^\perp), a(\chi_h)\big)^h .$$

We also consider the ratio

$$\mathfrak{r}^m = \frac{\max_{j=1,\ldots,J} |x_h^m(q_j) - x_h^m(q_{j-1})|}{\min_{j=1,\ldots,J} |x_h^m(q_j) - x_h^m(q_{j-1})|}$$

between the longest and shortest element of $\Gamma_h^m = x_h^m(I)$, and are often interested in the evolution of this ratio over time. We stress that no redistribution of vertices was necessary during any of our numerical simulations. We remark that a convergence experiment for (2.3), for an anisotropy of the form $\gamma(z,p) = \sqrt{p_1^2 + \delta^2 p_2^2}$ with $\delta > 0$, which confirms the theoretically obtained optimal H^1–error bound, can be found in [16, §6.1].

3.1. **The spatially homogeneous case.** In the case that

$$\gamma(z,p) = \gamma_0(p) \quad \text{and} \quad a(z) = 1 \qquad \forall\ z \in \Omega = \mathbb{R}^2 ,$$

for an anisotropy function $\gamma_0 \in C^2(\mathbb{R}^2 \setminus \{0\}, \mathbb{R}_{>0})$, the flow (1.6) reduces to classical anisotropic curvature flow, (1.5). Most existing approaches for the numerical approximation of anisotropic curve shortening flow deal with this simpler case, see e.g. [3, 5, 19, 31].

For our first experiment we choose the anisotropy from [19, (7.1)], with

$$\gamma_0(p) = |p|(1 + \delta\cos(k\theta(p))), \quad p = |p|\begin{pmatrix}\cos\theta(p)\\ \sin\theta(p)\end{pmatrix}, \quad k = 6,\ \delta = 0.028 , \tag{3.1}$$

and as initial curve use the one given in [28, p. 1494], i.e. we let

$$x(\rho, 0) = \begin{pmatrix}\cos u(\rho)\\ \frac12 \sin u(\rho) + \sin\left(\cos u(\rho)\right) + \sin u(\rho)\,[\frac15 + \sin u(\rho)\,\sin^2 u(3\rho)]\end{pmatrix}, \tag{3.2}$$

where $u(\rho) = 2\pi\rho$. The evolution is shown in Figure 1, where we can observe that the shrinking curve becomes convex, with its form soon approaching a scaled Wulff shape of the six-fold symmetric anisotropy (3.1). In addition, we once again note that the discrete energy $\mathcal{E}^h$ is monotonically decreasing, while the tangential motion induced by (1.10) leads to only a moderate initial increase in $\mathfrak{r}^m$, before it decreases towards the end.

With our next experiment we would like to demonstrate that our scheme can easily be extended to situations where a forcing term appears in the flow, e.g.

$$\mathcal{V}_\gamma = \varkappa_\gamma + f(\cdot, \nu) \qquad \text{on } \Gamma(t) , \tag{3.3}$$

in place of (1.4), where $f\colon \Omega \times \mathbb{R}^2 \to \mathbb{R}$. This leads to the additional term $\int_I f(x,\nu) H(x, x_\rho)\nu \cdot \eta \;\mathrm{d}\rho$ on the right hand side of (1.13), and analogously to

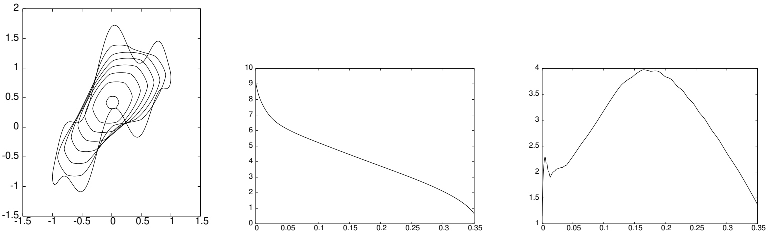

FIG. 1: Solution at times $t = 0, 0.05, \ldots, 0.35$. We also show a plot of the discrete energy $\mathcal{E}^h(x_h^m)$ (middle) and of the ratio $\mathfrak{r}^m$ over time (right).

the additional term $(f(x_h^m, \frac{(x_{h,\rho}^m)^\perp}{|x_{h,\rho}^m|})H(x_\rho^m, x_{h,\rho}^m)\frac{(x_{h,\rho}^m)^\perp}{|x_{h,\rho}^m|}, \eta_h)^h$ on the right hand side of (2.3). In our numerical experiments we choose

$$f(z,\nu) = f_0 \in \mathbb{R}\,,$$

so that (3.3) overall reduces to $\frac{1}{\gamma_0(\nu)}\mathcal{V} = \varkappa_{\gamma_0} + f_0$, compare with (1.5). Starting this flow from the same initial data (3.2), but now with the forcing $f_0 = 1.15$, leads to an expanding curve that, upon an appropriate rescaling, approaches the boundary of the Wulff shape, see Figure 2. What is particularly interesting in the observed evolution is that the ratio $\mathfrak{r}^m$ appears to tend towards unity, indicating an asymptotic equidistribution of the vertices on the polygonal curve.

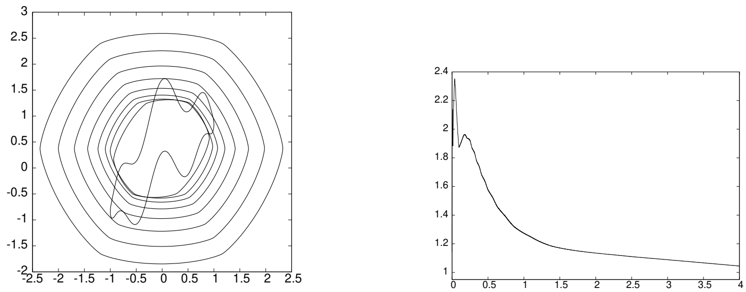

FIG. 2: Solution at times $t = 0, 0.5, \ldots, 4$. We also show a plot of the ratio $\mathfrak{r}^m$ over time.

3.2. **Geodesic curvature flow in Riemannian manifolds.** Let $(\mathcal{M}, g)$ be a two-dimensional Riemannian manifold, with local parameterization $F : \Omega \to \mathcal{M}$ and corresponding basis $\{\partial_1, \partial_2\}$ of the tangent space. We define

$$\gamma(z,p) = \sqrt{G^{-1}(z)p \cdot p} \quad \text{and} \quad a(z) = \sqrt{\det G(z)}.$$

Here, $G(z) = (g_{ij}(z))_{i,j=1}^2$, with $g_{ij}(z) = g_{F(z)}(\partial_i, \partial_j)$, $z \in \Omega$. Then (1.1) reduces to $\mathcal{E}(\Gamma) = \int_\Gamma \sqrt{G\tau \cdot \tau}\, \mathrm{d}\mathcal{H}^1$, the Riemannian length of the curve $\tilde{\Gamma} = F(\Gamma) \subset \mathcal{M}$, and it can be shown that (1.4) is now equivalent to geodesic curvature flow in $\mathcal{M}$, see [16, Appendix B] for details. Furthermore, in [16, §5.2] a possible construction of the splitting $\Phi_z^\pm$ is given, with the help of which the scheme (2.3) reduces to (5.10) in [16].

As an example we consider the case when $(\mathcal{M}, g)$ is a hypersurface in the Euclidean space $\mathbb{R}^3$. Assuming that $\mathcal{M}$ can be written as a graph, we let

$$F(z) = (z_1, z_2, \varphi(z))^T, \quad \varphi \in C^3(\Omega).$$

The induced matrix G is then given by $G(z) = \mathrm{Id} + \nabla\varphi(z) \otimes \nabla\varphi(z)$, and we have that $\Phi(z,p) = \frac{1}{2}G(z)p \cdot p$. For the splitting $\Phi = \Phi^+ + \Phi^-$ it is natural to let $\Phi^+(z,p) = \frac{1}{2}G_+(z)p \cdot p$, where $G_+(z) = G(z) + c_\varphi |z|^2 \mathrm{Id}$ and $c_\varphi \in \mathbb{R}_{\geq 0}$ is chosen sufficiently large. In our computation we observe a monotonically decreasing discrete energy when choosing $c_\varphi = 0$, and so we let $\Phi^+ = \Phi$.

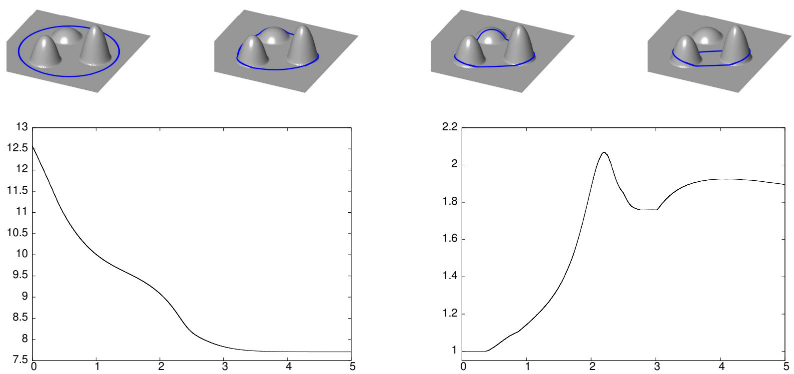

FIG. 3: Geodesic curvature flow on the graph defined by (3.4). We show the evolution of $F(x_h^m)$ on $\mathcal{M}$ at times $t = 0, 1, 2, 4$. Below we show a plot of the discrete energy $\mathcal{E}^h(x_h^m)$ (left) and of the ratio $\mathfrak{r}^m$ over time (right).

For our numerical simulation, following [33], we define a surface with three "mountains" via

$$\varphi(z) = \sum_{i=1}^{3} \lambda_i \psi(2|z - \mu_i|^2) \text{ with } \Omega = \mathbb{R}^2, \quad \text{where } \psi(s) = \begin{cases} e^{-\frac{1}{1-s}} & s < 1, \\ 0 & s \geq 1, \end{cases} \tag{3.4}$$

and where $\mu_1 = 0$, $\mu_2 = \binom{2}{0}$, $\mu_3 = \binom{1}{\sqrt{3}}$ and $(\lambda_1, \lambda_2, \lambda_3) = (1, 3, 4)$. On letting the initial polygonal curve be defined by an equidistributed approximation of a circle of radius 2 in Ω, centred at $\frac{1}{3}\sum_{i=1}^{3} \mu_i$, we show the evolution for geodesic curvature flow on the defined hypersurface in Figure 3. During the flow the curve tries to decrease its (Euclidean) length, while remaining on the manifold. As the initial circle begins to shrink, the curve is able to pass over the smallest of the three "mountains", but then reaches a steady state solution encompassing the two taller mountains. Here the curve cannot reduce its length further, because to rise higher up would yield an increase in its length, since it needs to remain attached to the flat part of the surface between the two mountains. We note that as soon as one of the larger "mountains" is not enclosed by the initial curve, then the evolution is going to lead to extinction in finite time. We show this in Figure 4, where the initial circle is now centred at $\binom{0}{\frac{1}{2}}$. Here the curve can continually decrease its length, until it reaches the peak of the tallest "mountain", where it shrinks to a point.

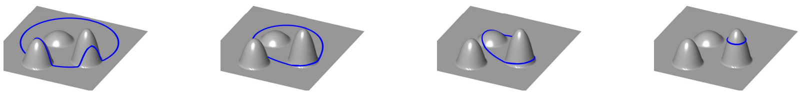

FIG. 4: Geodesic curvature flow on the graph defined by (3.4). We show the evolution of $F(x_h^m)$ on $\mathcal{M}$ at times $t = 0, 1, 2, 4$.

References

[1] Alfaro, M., Garcke, H., Hilhorst, D., Matano, H., Schätzle, R., *Motion by anisotropic mean curvature as sharp interface limit of an inhomogeneous and anisotropic Allen-Cahn equation*, Proc. Roy. Soc. Edinburgh Sect. A **140** (4) (2010), 673–706.

[2] Barrett, J.W., Blowey, J.F., *Finite element approximation of a model for phase separation of a multi-component alloy with non-smooth free energy*, Numer. Math. **77** (1) (1997), 1–34.

[3] Barrett, J.W., Garcke, H., Nürnberg, R., *Numerical approximation of anisotropic geometric evolution equations in the plane*, IMA J. Numer. Anal. **28** (2) (2008), 292–330.

[4] Barrett, J.W., Garcke, H., Nürnberg, R., *Numerical approximation of gradient flows for closed curves in* $\mathbb{R}^d$, IMA J. Numer. Anal. **30** (1) (2010), 4–60.

[5] Barrett, J.W., Garcke, H., Nürnberg, R., *The approximation of planar curve evolutions by stable fully implicit finite element schemes that equidistribute*, Numer. Methods Partial Differential Equations **27** (1) (2011), 1–30.

[6] Barrett, J.W., Garcke, H., Nürnberg, R., *Stable phase field approximations of anisotropic solidification*, IMA J. Numer. Anal. **34** (4) (2014), 1289–1327.

[7] Barrett, J.W., Garcke, H., Nürnberg, R., *Numerical approximation of curve evolutions in Riemannian manifolds*, IMA J. Numer. Anal. **40** (3) (2020), 1601–1651.

[8] Barrett, J.W., Garcke, H., Nürnberg, R., *Parametric finite element approximations of curvature driven interface evolutions*, Handb. Numer. Anal. (Bonito, A., Nochetto, R.H., eds.), vol. 21, Elsevier, Amsterdam, 2020, pp. 275–423.

[9] Bellettini, G., *Anisotropic and crystalline mean curvature flow*, A sampler of Riemann-Finsler geometry, Math. Sci. Res. Inst. Publ., vol. 50, Cambridge Univ. Press, 2004, pp. 49–82.

[10] Bellettini, G., Paolini, M., *Anisotropic motion by mean curvature in the context of Finsler geometry*, Hokkaido Math. J. **25** (3) (1996), 537–566.

[11] Beneš, M., Mikula, K., *Simulation of anisotropic motion by mean curvature-comparison of phase field and sharp interface approaches*, Acta Math. Univ. Comenian. (N.S.) **67** (1) (1998), 17–42.

[12] Caselles, V., Kimmel, R., Sapiro, G., *Geodesic active contours*, Int. J. Comput. Vis. **22** (1) (1997), 61–79.

[13] Clarenz, U., Dziuk, G., Rumpf, M., *On generalized mean curvature flow in surface processing*, Geometric Analysis and Nonlinear Partial Differential Equations, Springer-Verlag, Berlin, 2003, pp. 217–248.

[14] Deckelnick, K., Dziuk, G., *On the approximation of the curve shortening flow*, Calculus of Variations, Applications and Computations (Pont-à-Mousson, 1994) (Bandle, C., Bemelmans, J., Chipot, M., Paulin, J.S.J., Shafrir, I., eds.), Pitman Res. Notes Math. Ser., Longman Sci. Tech., Harlow, 1995, pp. 100–108.

[15] Deckelnick, K., Dziuk, G., Elliott, C.M., *Computation of geometric partial differential equations and mean curvature flow*, Acta Numer. **14** (2005), 139–232.

[16] Deckelnick, K., Nürnberg, R., *A novel finite element approximation of anisotropic curve shortening flow*, arXiv:2110.04605 (2021).

[17] Deimling, K., *Nonlinear functional analysis*, Springer-Verlag, Berlin, 1985.

[18] Dziuk, G., *Convergence of a semi-discrete scheme for the curve shortening flow*, Math. Models Methods Appl. Sci. **4** (4) (1994), 589–606.

[19] Dziuk, G., *Discrete anisotropic curve shortening flow*, SIAM J. Numer. Anal. **36** (6) (1999), 1808–1830.

[20] Ecker, K., *Regularity Theory for Mean Curvature Flow*, Birkhäuser, Boston, 2004.

[21] Elliott, C.M., Fritz, H., *On approximations of the curve shortening flow and of the mean curvature flow based on the DeTurck trick*, IMA J. Numer. Anal. **37** (2) (2017), 543–603.

[22] Elliott, C.M., Stuart, A.M., *The global dynamics of discrete semilinear parabolic equations*, SIAM J. Numer. Anal. **30** (6) (1993), 1622–1663.

[23] Garcke, H., Lam, K.F., Nürnberg, R., Signori, A., *Overhang penalization in additive manufacturing via phase field structural topology optimization with anisotropic energies*, arXiv:2111.14070 (2021).

[24] Giga, Y., *Surface evolution equations*, vol. 99, Birkhäuser, Basel, 2006.

[25] Gurtin, M.E., *Thermomechanics of Evolving Phase Boundaries in the Plane*, Oxford Mathematical Monographs, The Clarendon Press Oxford University Press, New York, 1993.

[26] Haußer, F., Voigt, A., *A numerical scheme for regularized anisotropic curve shortening flow*, Appl. Math. Lett. **19** (8) (2006), 691–698.

[27] Mantegazza, C., *Lecture notes on mean curvature flow*, Progress in Mathematics, vol. 290, Birkhäuser/Springer Basel AG, Basel, 2011.

[28] Mikula, K., Ševčovič, D., *Evolution of plane curves driven by a nonlinear function of curvature and anisotropy*, SIAM J. Appl. Math. **61** (5) (2001), 1473–1501.

[29] Mikula, K., Ševčovič, D., *A direct method for solving an anisotropic mean curvature flow of plane curves with an external force*, Math. Methods Appl. Sci. **27** (13) (2004), 1545–1565.

[30] Mikula, K., Ševčovič, D., *Computational and qualitative aspects of evolution of curves driven by curvature and external force*, Computing Vis. Sci. **6** (4) (2004), 21–225.

[31] Pozzi, P., *Anisotropic curve shortening flow in higher codimension*, Math. Methods Appl. Sci. **30** (11) (2007), 1243–1281.

[32] Taylor, J.E., Cahn, J.W., Handwerker, C.A., *Geometric models of crystal growth*, Acta Metall. Mater. **40** (7) (1992), 1443–1474.

[33] Wu, C., Tai, X., *A level set formulation of geodesic curvature flow on simplicial surfaces*, IEEE Trans. Vis. Comput. Graph. **16** (4) (2010), 647–662.

Institut für Analysis und Numerik,
Otto-von-Guericke-Universität Magdeburg,
39106 Magdeburg, Germany
E-mail: klaus.deckelnick@ovgu.de

Dipartimento di Mathematica, Università di Trento,
38123 Trento, Italy
E-mail: robert.nurnberg@unitn.it